



# 第五十屆電子元件及技術會議

交通大學 邱碧秀

## 1. 參加會議經過

第五十屆電子元件及技術會議 (50<sup>th</sup> Electronic Components and Technology Conference, 50<sup>th</sup> ECTC) 於 2000 年 5 月 21 日至 24 日在美國內華達州拉斯維加斯舉行。由國際電子電機協會 (IEEE, CPMT) 及電子元件組裝和材料協會 (ECA) 舉辦。此研討會的主題是和電子構裝有關的材料、元件及製程技術。國內出席本次會議者，除筆者外，尚有成功大學林光隆教授、中山大學鄭木海教授、電信研究所及工業技術研究院的相關研究群及數位國內業者。

## 2. 與會心得

會議分 38 個議程舉行，由於議程太多，很多精采的論文無法參與，覺得很可惜。筆者以往參加國際會議都是找和自己研究領域相近的論文聽。這次因為和自己研究領域相近的議程太多，時間上相互衝突，難以取捨。故乾脆參加自己較生疏的領域的議程。三天半下來。倒也頗有斬獲。另外，筆者的論文 “Electromigration in Sputtered Copper Interconnection with Polyimide as Interlevel Dielectric or Passivation” 是在 24 日下午，以海報形式發表。觀眾反應熱烈，會後收到不少 e-mail 討論相關問題。充分達到溝通討論之效。

此次會議最大的缺點就是會議地點在賭城。每次進出開會地點都

會經過旅館的賭場，空氣不好，光線陰暗又吵雜，感覺很不舒服。

此行帶回會議論文集一冊，並買了幾本今年度出版的電子構裝方面的書籍，可供日後教學及研究參考。

### **3. 建議**

ECTC 會議的研討重點是電子構裝方面，是電子產業中非常重要的一環，希望政府能多鼓勵及資助相關學者參與此類會議。另外，非常感謝國科會的補助，讓我得以成行。

# Electromigration in Sputtered Copper Interconnection with Polyimide as Interlevel Dielectric or Passivation

Bi-Shiou Chiou, Jiann-Shan Jiang, Hsueh-Wen Wang, and Han-Yi Hung  
 Department of Electronics Engineering and Institute of Electronics,  
 National Chiao-Tung University, 1001 Ta Hsueh Road, Hsinchu, Taiwan  
 E-mail bschiou@cc.nctu.edu.tw

### Abstract

Electromigration damage (EMD) is one of the major causes for the failures of interconnection. The use of copper and low dielectric constant dielectric has been proposed to reduce the RC time delay and to improve EMD. In this study, the Electromigration of Cu with polyimide is investigated with an empirical formula

$$\frac{dR}{dt} \cdot \frac{1}{R_0} = AJ^n \exp\left(-\frac{Q}{RT}\right)$$

Secondary ion mass spectrometry (SIMS) reveals the interdiffusion between Cu and polyimide during curing of the polyimide and/or annealing of Cu metallization. Thin layers of TiW is deposited between polyimide and Cu as a barrier to reduce the interdiffusion. The activation energy Q for the electromigration of Cu on polyimide is 0.77eV from 120°C to 230°C, while activation energies for samples with titanium tungsten as an interlayer are 0.79eV (140°C to 190°C) and 1.73eV (190°C to 230°C). The presence of TiW barrier enhances the high temperature electromigration resistance and promotes the adhesion between Cu and polyimide interface. However, films with TiW are found to be more sensitive to current stressing than those without.

Polyimide is also employed as a passivated layer on top of Cu metallization. Resistance of the passivated samples decrease in the initial stage of the electromigration experiment. Possible causes are discussed on the decrease in R.

The geometry of the metallization also affects the electromigration, the current exponent (n), calculated from EMD data, are different for interconnection with different geometries.

### Introduction

Copper, with its low resistivity, high melting point, and high mechanical strength, has been considered as a substitute for Al interconnection in VLSI devices. Electro migration damage (EMD) in Al or Al alloy has been known to be a primary reason for circuit failure [1]. Although Cu has higher resistance to EMD than Al, the deficiencies of copper, such as: poor adhesion to the dielectric layers, uncontrollable dry etching, lack of self-passivation oxide and environmental reactivity limit the application of copper in IC fabrications. The poor adhesion can be improved by adding diffusion barrier as an underlying layer.

Scaling of ultra large-scale integrated (ULSI) circuits to dimensions under 0.5 μm has placed a considerable burden on the thin film interconnections. One of the most important phenomena affecting the reliability of fine-line metal interconnection is electromigration, which occurs when high electron currents (10<sup>5</sup>-10<sup>6</sup> A/cm<sup>2</sup>) drive atoms from the cathode end of the metallization toward the anode end and results in structural damage such as voids and hillocks. Hence,

thin film metallizations are usually coated with passivation layer which refrain the atom diffusion by restricting the accumulation of mass and thereby diminishing the mass flow. It has been shown that the presence of a dielectric overcoat can significantly affect the extent of electromigration damage in Al and Al(Cu) conductors[2-6].

In this research, the electromigration in DC sputtered copper interconnect with polyimide as interlevel dielectric or passivation layer is investigated. The high thermal stability, ease of planarization, low processing temperature and low dielectric constant render polyimide a good candidate as dielectric material for multilayer-structure devices. The barrier effect of TiW on electromigration in sputtered Cu film on polyimide is also studied. The kinetics of electromigration damage are studied by an isothermal resistance change analysis method utilizing an empirical formula,

$$\frac{dR}{dt} \cdot \frac{1}{R_0} = AJ^n \exp\left(-\frac{Q}{RT}\right) \quad (1)$$

The activation energy Q for EMD and the exponent (n) of the current density are calculated and discussed.

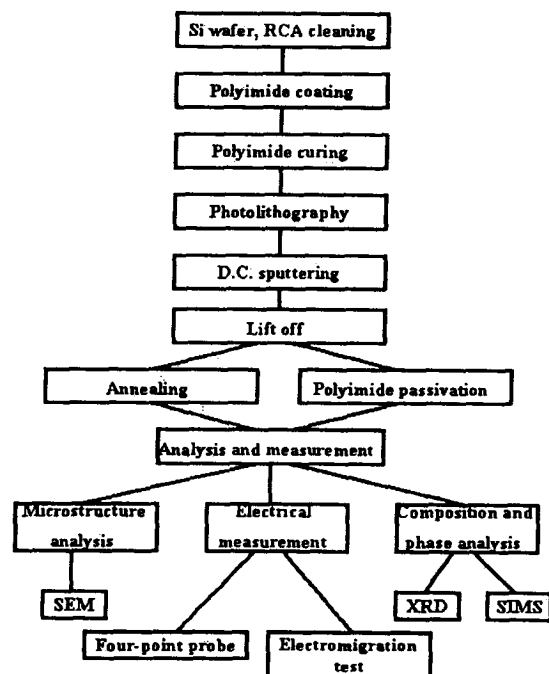


Fig. 1 Flow Chart of Experimental Procedures.

## Experimental Procedures

Fig.1 gives flow chart of the experimental sequence. Copper film was sputtered onto polyimide coated Si substrate. P-type (100) oriented Si wafers with nominal resistivity of 1 to 10  $\Omega$ -cm (Topsil Inc., USA) were employed. The Si wafers were cleaned with standard RCA cleaning process.

Polyimide 2540 (Pyralin, Du pont, USA), polyamic acid, was statically dispensed and spun on Si wafers with a conventional spin coater (Spinner, Synrex, Taiwan). The spinning process consisted of two steps. The first step, known as dispense-and-spread cycle, is 20 sec. at 1000rpm. The second step which determines polyimide films thickness is 30 sec. at 4500 rpm.

Curing (completely imidized) of polyimide was carried out in a quartz tube with nitrogen ambient to prevent the polyimide from degradation. The nitrogen flow rate was 1416 standard centimeter cubic per minute (sccm, i.e., 3 cubic ft/hr). the curing conditions are: 2°C/min from 25°C to 110°C, 30 min at 110°C, 2°C/min from 110°C to 230°C, 60 min at 230°C, 5°C/min from 230°C to 420°C, and 420°C for 60 min. The film thickness of the cured polyimide is  $\sim 3 \mu\text{m}$ .

The polyimide coated Si substrate was processed using conventional photolithography to obtain the test pattern. Samples with positive photoresist patterns were transferred to a vacuum chamber for the sputtering of Cu and TiW films. High purity Ar gas was introduced through a mass flow controller after the vacuum was evacuated to about  $10^{-6}$  torr. The flow rate of Argon was 24 sccm. The sputtering targets were a 99.995% Cu disc (diameter: 15.24cm<sup>2</sup>, thickness: 0.3cm, Plasmaterials Inc., USA) and Ti: W = 10: 90 wt% or a Ti<sub>0.3</sub>W<sub>0.7</sub> disc of 99.9% purity (diameter: 15.24cm<sup>2</sup>, thickness: 0.3cm, Cerac Inc., USA). Before deposition, the target was pre-sputtered for 1 min. to remove any contaminate. The gas pressure was kept at  $2 \times 10^{-3}$  torr and the sputtering power employed during deposition was between 60W to 300W. The distance between sample and target ranged from 9.5cm to 30cm. Copper was sputtered after TiW deposition without breaking the vacuum. A Lift-off process was carried out after the sputtering of TiW and Cu to leave a pattern for EMD tests. After the lift-off process, samples were annealed at 250°C, 400°C, or 420°C for 30 minutes.

The film thickness was measured with a stylus surface profiler. The sheet resistance of the samples was measured with a four-point probe. An X-ray diffractometer was used to identify the crystalline phase of the films. The microstructure of the sample was examined with a field emission scanning microscope (FESEM, S-4000, Hitachi, Japan) and a transmission electron microscope. An optical microscope was employed to examine samples after development and lift-off. Auger electron spectroscopy (PERKIN PHI-590AM, Massachusetts, USA) was used to analyze the concentration profile of the films. The electromigration tests were carried out in a quartz tube at temperatures ranging from 110°C to 230°C in a N<sub>2</sub> atmosphere. The four I/O pads of the samples were connected to a constant current source (Model 220, Keithley, USA) and a micro-voltage meter (Model 197, Keithley, USA).

The leads between the samples and measurement system were covered with aluminum foil to avoid external electro-

magnetic interference. The voltage was acquired once per minute or per 10 minutes automatically. The resistance was obtained by dividing the voltage by the current.

Thermal analyses including thermogravimetry analysis (TGA), differential thermal analysis (DTA), differential scanning calorimetry (DSC) and differential of differential scanning calorimetry (DDSC) were also carried out to analyze the curing process of polyimide.

## Results and Discussion

Figures 2 and 3 show the DSC and DDSC curves of polyimide in air ambient. The DDSC curve suggests that curing of PI starts at  $\sim 169^\circ\text{C}$  and completed at  $\sim 202^\circ\text{C}$ . This is consistent with the infrared spectrum of polyimide[7].

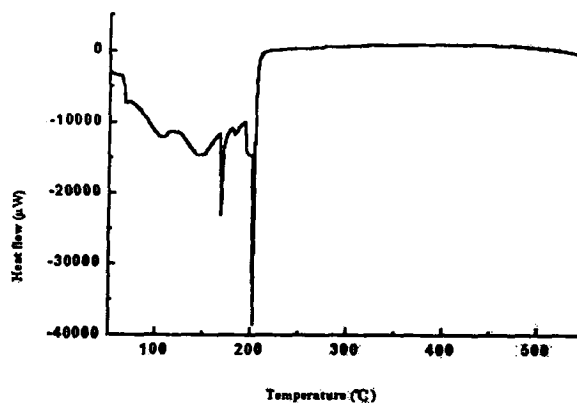


Fig. 2 DSC curve of polyimide in air ambient.

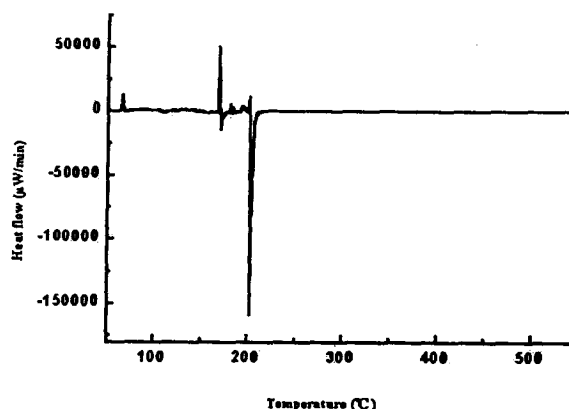


Fig. 3 DDSC curve of polyimide in air ambient.

Copper films prepared in the study have a TCR ranging from 2750 ppm/K to 3500 ppm/K and a resistivity between  $1.8 \mu\Omega\text{-cm}$  to  $2.38 \mu\Omega\text{-cm}$ , depending on the sputtering conditions. X-ray diffraction results indicate that both the as-deposited and the annealed Cu films are crystalline phases.

The kinetics of electromigration damage is studied with an isothermal resistance change analysis method. Fig.4 exhibits the relative resistance  $R/R_0$  of Cu film on polyimide with or without TiW barrier layer as a function of time at various temperatures. The resistance increases more rapidly at higher soaking temperatures. By defining a resistance change of

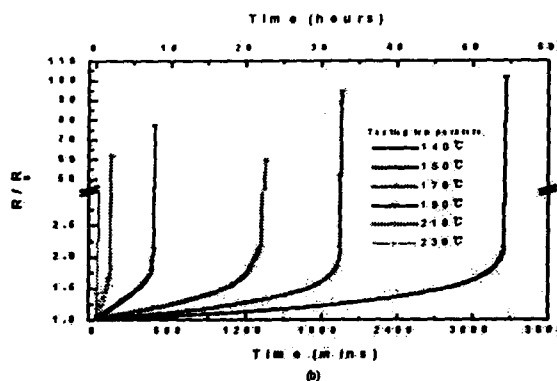
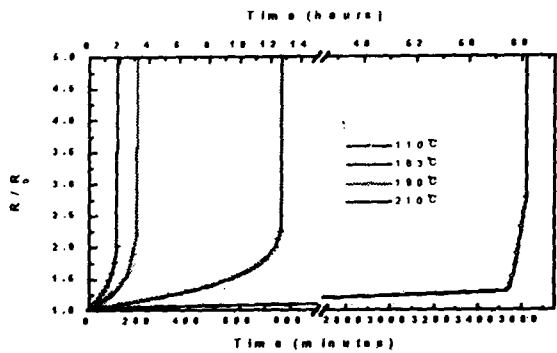


Fig. 4 Relative resistance  $R/R_0$  as a function of time for copper on polyimide (a) without and (b) with TiW barrier layer.  $J=1.31\text{MA}/\text{cm}^2$ .

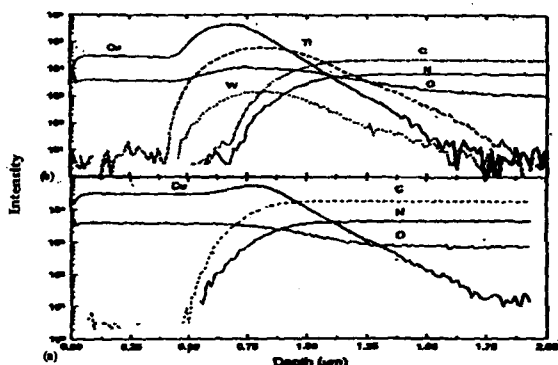


Fig. 5 SIMS depth profile of Cu film on polyimide (a) without and (b) with TiW barrier layer. Films annealed at  $400^\circ\text{C}$  for 30 min.

4.5% as the criterion of early stage failure, i.e. assuming the dimensions of the maximum voids are much less than the line width, the time rate change of electrical resistance  $dR/dt$  due to the electromigration damage is thermally activated and the activated energy can be calculated with Eq. (1). The activation energy for Cu film on polyimide is  $0.77\text{eV}$  ( $110^\circ\text{C}$  to  $220^\circ\text{C}$ ),

while two activation energies,  $1.73\text{eV}$  ( $190^\circ\text{C}$  to  $230^\circ\text{C}$ ) and  $0.79\text{eV}$  ( $140^\circ\text{C}$  to  $190^\circ\text{C}$ ), are obtained for Cu film with TiW barrier layer. The presence of two activation energies suggests a surface electromigration mechanism at low temperatures and a combined migration mechanism at high temperatures. SIMS depth profiles, shown in Fig.5, indicate that TiW film blocks the interdiffusion between Cu and polyimide. This could be one of the reasons that the presence of TiW barrier layer improves the high temperature electromigration resistance.

The adhesion strength of Cu on polyimide is  $0.82\pm 0.19\text{kg}/\text{mm}^2$ . Addition of TiW barrier layer between copper and polyimide enhances the adhesion strength to  $1.01\pm 0.19\text{kg}/\text{mm}^2$ .

The current exponent  $n$  in Eq. (1), calculated from the EDM data is 5.41 for Cu/TiW as compared to 3.58 for Cu, indicating that Cu/TiW is more sensitive to current stressing than Cu. Values of  $n$  greater than 2 can probably be attributed to Joule heating effects which result in a temperature gradient-induced flux divergence. Some models predicted values of 1 to 15 depending on Joule heating. The thermal conductivities of both Ti ( $22\text{W}/\text{m}\cdot\text{K}$ ) and W ( $167\text{W}/\text{m}\cdot\text{K}$ ) are much smaller than that of Cu ( $395\text{W}/\text{m}\cdot\text{K}$ ). Besides, the resistivity of TiW film ( $\sim 104\ \mu\Omega\cdot\text{cm}$ ) is much larger than that of Cu. One would expect that the introduction of the TiW barrier layer degrades the power dissipation ability of Cu films and results in a larger  $n$ . However, there are many factors, such as: electric field, temperature gradient, residual stress, etc., which would influence the migration of Cu. The root causes for the increase of  $n$  are yet to be revealed.

The effect of polyimide passivation on the electromigration of Cu is studied. Fig.6 exhibits the typical relative resistance change as a function of current stressed time for copper on polyimide passivated with polyimide (i.e., PI/Cu/PI/Si). An initial decrease followed by an increase of the resistance is observed. There are many possibilities which would cause the drop in  $R$ , such as: Joule heating, solute segregation-etc.. The TCR of Cu film in this study ranges from  $2750\text{ppm}/\text{K}$  to  $3500\text{ppm}/\text{K}$ . For a TCR of  $3500\text{ppm}/\text{K}$ , the temperature on the test line raises  $\sim 125^\circ\text{C}$  at a current density of  $3.42\text{MA}/\text{cm}^2$ . As the film was annealed at  $420^\circ\text{C}$  before electromigration test,  $125^\circ\text{C}$  is not high enough to cause the resistance drop. Hence, Joule heating is not the major cause for decrease in  $R$ . SIMS depth profile, shown in Fig.5, reveals the interdiffusion between polyimide and copper interface. The depletion of the impurities (C, N) in Cu grain is one possibility that causes the decrease in resistance. A polyimide passivation on the test line provides an ample source of impurity so the  $R$ -decrease of the passivated sample is observed.

The geometry of the metallization also affects the electromigration. Cu metallizations with zigzag patterns were fabricated and the EMD tested. The activation energy of a zigzag Cu film ( $0.5\text{eV}$ ) is smaller than that of a straight one ( $0.77\text{eV}$ ). Electromigration occurs at high currents, a bend in metallization results in current crowding and, consequently, reduces the activation energy of the zigzag film. The current exponent for the zigzag film is 3.35, which is comparable to that of straight Cu film (3.58).

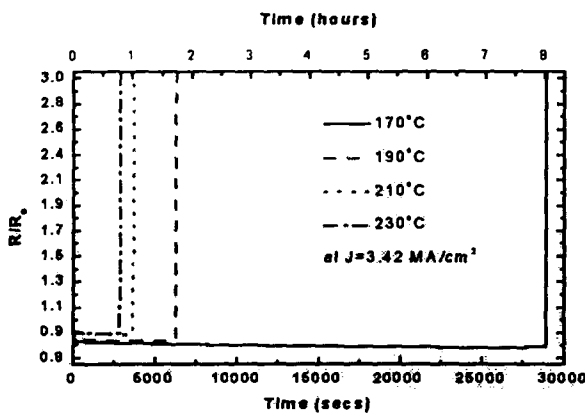


Fig. 6 Relative resistance  $R/R_0$  as a function of time for copper passivated with polyimide.

### Conclusions

1. The electromigration resistance of Cu on polyimide can be enhanced with the addition of TiW barrier layer. The presence of TiW retards the interdiffusion between Cu and polyimide, raises the activation energy for the electromigration of Cu, and, enhances the adhesion strength between Cu and polyimide.
2. Passivation of Cu film with polyimide causes a drop in resistance in the early stage of electromigration test. Interdiffusion between Cu and polyimide during annealing results in the resistance drop.
3. Current crowding affect Cu migration and should be avoided in the design of a reliable interconnect.

### Acknowledgment

This work is sponsored by National Science Council, Taiwan, under the contract numbers NSC87-2218-E-009-031 and NSC86-2221-E-009-062.

### References

1. C.K. Hu and J.M.E. Harper, "Copper interconnection and reliability", *Materials Chemistry and Physics*, Vol.52, pp.5-16, 1998.
2. S. Foley, A. Ryan, D. Martin and A. Mathewson, "A study of the influence of inter-metal dielectrics on electromigration performance", *Microelectronics Reliab.*, Vol.38, No.1, pp.107-113, 1998.
3. J.R. Lloyd, "Electromigration in Al-Cu thin films with polyimide passivation", *Thin Solid Films*, Vol.91, pp.175-182, 1982.
4. B.H. Jo and R.W. Vook, "In-situ ultra-high vacuum studies of electromigration in copper films", *Thin Solid Films*, Vol.262, pp.129-134, 1995.
5. J.R. Lloyd and P.M. Smith, "The effect of passivation thickness on the electromigration lifetime of Al-Cu thin film conductors", *J. Vac. Sci. Technol.*, Vol. A1, No.2, pp.455-458, 1983.
6. H.A. Schafft, C.D. Younkens and T.C. Grant, "Effect of passivation and passivation defects on electromigration failure in aluminum metallization", *IEEE/IRPS*, pp.250-255, 1984.
7. H.Y. Hung, "The poison effect on Cu electromigration degradation", Master's thesis, National Chiao Tung University, Taiwan, June, 1999.



**COLOR**

The CD-ROM version of this paper contains color, to assist you in interpretation.  
<http://www.cpmt.org/proceedings/order.html>

# 高密度多層構裝基板與接合材料研究-子計畫二： 銅接合-低介電係數介電層之界面可靠度提昇研究

計畫編號: NSC 89-2216-E-009-017

執行期限: 88年8月1日至89年7月31日

子計畫主持人: 邱碧秀 國立交通大學電子工程學系

總計畫主持人: 邱碧秀 國立交通大學電子工程學系

## 一、中文摘要

隨著元件尺寸的縮小, RC 延遲限制了電路的傳輸速度。解決方式便是使用低介電材料如 HSQ (hydrogen silsesquioxane) 和低阻率的銅。在本實驗中, 主要探討擴散層鈦(Ta)在 HSQ 和 SiO<sub>2</sub> 基材上對銅遷移的影響。而且, 對 Cu/Ta 金屬膜在 HSQ 和 SiO<sub>2</sub> 基材上的特性及 HSQ 的熱學性質也有所探討。從 TG/DTA, FTIR 和折射率分析, 固化溫度在 400 °C 可以獲得較低的介電常數。使用擴散層鈦(Ta)不但可以改善銅和 HSQ 的接合強度, 而且可以阻擋銅擴散到 HSQ 中。並且, 擴散層鈦(Ta)可以改善銅的結晶性, 進而增強銅在高溫下的電致遷移。另外, 比較銅/鈦(Cu/Ta)金屬膜在 HSQ 和 SiO<sub>2</sub> 基材上的特性和電遷移的影響, 發現 HSQ 基材的粗糙度和氫會影響銅/鈦(Cu/Ta)金屬膜的阻率和抗電致遷移的能力。除此之外, 在高電流密度下, 具有較差的熱傳導係數的 HSQ 會導致嚴重的焦耳效應, 進而降低抗電致遷移的能力。

## Abstract

As device scaling down to sub-micron, the RC time delays become the limitation to circuit speed. The solution is the use of low dielectric materials (such as HSQ) and low resistivity materials (such as copper). In this work, the influence of underlying barrier Ta on Cu electromigration (EM) performance for HSQ and SiO<sub>2</sub> substrate was investigated. The properties of Cu/Ta on HSQ coated Si substrate and the thermal properties of HSQ were also studied. From TG/DTA, FTIR, and refractive index analysis, curing at around 400°C is desired to obtain lower dielectric constant property. The presence of a Ta barrier not only improves the adhesion between Cu and dielectrics, but also blocks the Cu diffusion into dielectrics. And the presence of a Ta barrier can enhance the microstructure and improve the Cu electromigration at high temperatures. The hydrogen from HSQ may affect the resistivity of metal films and electromigration performance. The roughness of HSQ may influence the resistivity of metal films for as-deposited condition. The poor thermal conductivity of HSQ substrate enhances Joule heating effects and then degrades the EM performance.

## 二、緣由與目的

隨著元件尺寸的縮小, 導線傳輸延遲時間成為電路速度的限制。為了解決這樣的問題, 使用低阻率和低

介電材料成為未來 IC 的趨勢。

銅是一個不錯的材料, 因為它具有較低的阻率 (1.7  $\mu\Omega$  cm) 且抗電致遷移能力比鋁還要好[1]。然而, 使用銅會有一些問題, 如它很容易氧化, 與低介電材料接合差, 易擴散到矽基材等缺點。

在低介電材料的選擇方面, HSQ 應用在 IC 製程上是一個不錯的材料, 因為它具有低介常數, 不含碳, 非回蝕製程, 較佳的填洞能力, 平坦度佳等優點。不過, HSQ 目前仍有一些製程整上的問題, 如 Si-H 熱分解, 氧化, 電漿破壞等[2]。

本計劃使用 HSQ 來當作低介電材料, 並探其熱學性質。使用擴散阻擋層鈦(Ta)來改善銅和低介電材料的接合強度。另外, 對 HSQ 和擴散阻擋層鈦(Ta)對銅電致遷移的可靠度影響亦有所探討。

## 三、結果與討論

### 3-1 HSQ(hydrogen silsesquioxane)的熱學性質

圖 1 為 HSQ 在氮氣的環境下, 加熱速率每分鐘 10 度的熱重熱差分析(TG/DTA)曲線圖。從 TG 圖, 可看出溫度小於 200°C 時, 重量損失大約 3%。且 DTA 分析, 吸熱反應在 32°C 左右。這表示 HSQ 在小於 200°C 的反應為溶劑揮發。而在 400°C 左右時, 重量突然減少且放熱反應在 400°C 左右, 表示 HSQ 在 400°C 上下發生結構上的變化並釋放出氣體。

圖 2 為 HSQ 在不同固化溫度的傅立葉轉換紅外光譜(FTIR)。從圖 2 來比較在 Si-O(1130  $\text{cm}^{-1}$ ) 拉伸鍵結, Si-O(1070  $\text{cm}^{-1}$ ) 網狀拉伸鍵結, 及 Si-H(2250  $\text{cm}^{-1}$ ) 拉伸鍵結, 可得知固化溫度在 350°C 時, HSQ 的結構為籠狀結構 (cake-like structure)。固化溫度在 400°C 時, Si-O 網狀拉伸鍵結強度增強, 且 Si-O 籠狀拉伸鍵結強度及 Si-H 拉伸鍵結減弱, 表示 HSQ 膜在 350 至 400°C, 從籠狀結構變為網狀結構且釋放出氫氣或矽甲烷氣體[3]。然而, 在 450°C 時, 由於熱解分解導致 Si-H 的強度減弱, 所形成的 Si 懸鍵, 重新鍵結形成較強的 Si-Si 共價鍵結[4]。當 Si-H 被破壞時, HSQ 膜將變得致密。此表示在 450°C, HSQ 具有較高的密度和介電常數, 因為較強的 Si-H 鍵及孔洞結構是維持低介電係數的兩個主要因子。這可從折射率分析來得知。

圖 3 為 HSQ 膜在不同固化溫度的折射率及光學介電常數。在 350°C, HSQ 的折射率為 1.372, 光學介電常數為 1.882。而當固化溫度在 400°C, HSQ 的折射率降為 1.365, 光學介電常數為 1.863。而在 450°C, 折射率反而增至 1.383, 光學介電常數為 1.913。這和 FTIR 的分析



相符，因為固化溫度為 350°C 時，HSQ 的結構為籠狀結構，具有較高的密度及折射率；固化溫度為 400°C，HSQ 的結構為網狀結構，具有較低的密度及折射率。然而，在固化溫度在 450°C，折射率會再上升的原因，跟 HSQ 的 Si-H 鍵熱分解導致薄膜變得致密有關。

### 3-2 擴散阻擋層鈿(Ta)對 Cu/Ta/SiO<sub>2</sub> 結構的影響

銅很容易擴散至介電材料且與其接合很差[5]。因此，銅需要一層擴散阻擋金屬來防止銅擴散至介電材料且改善彼此之間的接合強度。在沒有加擴散阻擋層鈿(Ta)時，銅和二氧化矽(SiO<sub>2</sub>)的接合強度為 1.42 ± 0.25 kg/mm<sup>2</sup>。然而，在加了金屬鈿後，接合強度變為 31.35 ± 3.24 kg/mm<sup>2</sup>。所以，差的接合強度可以經由加入金屬鈿而獲得改善。另外，金屬鈿亦可阻銅擴散至介電材料中，如圖 4 所示

在電致遷移方面，金屬鈿擔任一個重要的角色，因為它不但可以改善銅膜的微結構且可以增強銅的抗電遷移能力[6,7]。在量測電致遷移前，首先要評估焦耳熱對銅線溫度的修正。這可經由量測電阻對溫度變化及電阻對電流之圖而獲得在不同電流密度所引起的溫度上升。

溫度係數(TCR)定義為  $TCR = \frac{1}{R_0} \cdot \frac{R - R_0}{T - T_0}$ ，其中

$R_0$  為  $T_0$  之電阻。如圖 5 所示，所求溫度係數為  $3.53 \times 10^{-3} 1/^\circ\text{C}$ 。結合圖 6 便可獲得由焦耳熱引起銅線之溫度上升，如圖 7 所示。在電流密度為 5 MA/cm<sup>2</sup>，溫度大約上升 8°C 左右。圖 8 為電流密度 5 MA/cm<sup>2</sup>，不同溫度下，相對電阻對時間的變化。定義相對電阻變化 4.5% 為元件失效時間，且使用經驗公

$$[8-10] \frac{dR}{dt} \cdot \frac{1}{R_0} = AJ^n \exp\left(-\frac{Q}{kT}\right)$$

來求得活化能 Q 值，其中

A=與金屬薄膜特性相關之結構常數

J=電流密度(A/cm<sup>2</sup>)

n=電流密度加速因子

Q=活化能(eV)

K=波茲曼常數

$8.62 \times 10^{-5} \text{ eV/K}$

T=絕對溫度(K)

在低溫範圍(225~250°C)，Q 值為 0.54 eV，在高溫範圍(275~300°C)，Q 值為 2.09 eV，如圖 9(a)所示。這表示在低溫可能的電遷移機制為經由表面擴散，而在高溫為晶格擴散。若為最佳直線，Q 值為 1.14 eV 如圖 9(b) 所示。表示其擴散機制是經由晶界來擴散。

### 3-3 HSQ 對 Cu/Ta/HSQ 結構的影響

在剛沈積時，Cu/Ta 金屬膜的阻率在二氧化矽(SiO<sub>2</sub>)和 HSQ 基材上分別為 4.13 μΩ·cm 和 5.24 μΩ·cm。Cu/Ta 金屬膜的阻率在二氧化矽(SiO<sub>2</sub>)比在 HSQ 低。可能的原因有很多。其中表面的粗糙度可能是重要的因子，因為二氧化矽的粗糙度比 HSQ 小，如圖 10 所示。且比較 Cu/Ta 金屬膜在不同基材的 XRD 銅(111)，如圖 11 所示，發現銅在二氧化矽的結晶比在 HSQ 的還要好，結晶比較好的，相對阻率會比較低。文獻已報導較粗糙的表面，會有較高的阻率[11,12]。然而，在退火後，Cu/Ta 金屬膜的阻率在 HSQ 反而比在二氧化矽還要低。可能

的原因不只一個。根據阻率分析，電阻率可分為溫度相關和與溫度無關兩項。在相同溫度下，由聲子引起的阻率貢獻相同。所以，其主要差異應在與溫度無關的阻率上。圖 12 為 Cu/Ta/HSQ 結構在退火後，可能產生的化學反應，相轉換及其所在位置。由圖 13 顯示沒有化合物的形成。且文獻亦報導銅，鈿的矽化物形成溫度在 600°C[13]。而且，鈿不跟銅產生反應[14]，也沒有鈿的相轉換因為在 500~800°C 退火，才會有相轉換的發生[15]。因此，可能是氫雜質擴散至金屬中，如圖 14 所示。在文獻有報導氫會使電阻率下降[16,17]。所以，氫可能是導致 Cu/Ta 金屬膜在 HSQ 基材上電阻率較低的原因。

在電致遷移量測方面，使用 HSQ 當基材的結構 Cu/Ta/HSQ/Si 求得之活化能 Q 為 1.10 eV，如圖 15 所示，在電流密度 5MA/cm<sup>2</sup>，銅線上升溫度約為 15 度。與使用二氧化矽當基材的結構 Cu/Ta/SiO<sub>2</sub>/Si 比較，在活化能之值兩者差不多，生命期則是二氧化矽為基材的比較長。這個原因可能是因為二氧化矽具有較低的熱導率所致。

## 四、結論

從 HSQ 的熱分析，可以得知 HSQ 的溶劑在 200°C 內揮發。固化溫度在 350°C，薄膜是籠狀結構。固化溫度在 400°C，薄膜是網狀結構。固化溫度在 450°C，則薄膜變得致密。在金屬鈿的影響方面，鈿不但可以改善接合強度，也可阻止銅的擴散。並且，擴散層鈿(Ta)可以改善銅的結晶性，進而增強銅在高溫下的電致遷移。在 HSQ 的影響方面，在高電流密度下，具有較差的熱傳導係數的 HSQ 會導致嚴重的焦耳效應，進而降低抗電致遷移的能力。

## 五、參考文獻

- [1] T. Nitta, T. Ohmi, T. Takewaki and T. Shibata, "Electrical properties of giant-grain copper thin films formed by a low kinetic energy particle process", *Journal of the Electrochemical Society*, Vol.139, No.3, pp. 922-927, March 1992.
- [2] M.J. Loboda, and G.A. Toskey, "Understanding hydrogen silsesquioxane-based dielectric film processing", *Solid State Technology*, Vol. 41, No. 5, pp. 99-102, May 1998.
- [3] M.G. Albrecht, and C. Blanchette, "Materials issues with thin film hydrogen silsesquioxane low K dielectrics", *Journal of the Electrochemical Society*, Vol. 145, No. 11, pp.4019-4025, November 1998.
- [4] A. Courtot-Descharles, F. Pires, P. Paillet, J.L. Leray, "Density functional theory applied to the calculation of dielectric constant of low-k materials", *Microelectronics Reliability*, Vol. 39, pp. 279-284, 1999.
- [5] C.-K. Hu, B. Luther, F.B. Kaufman, J. Hummel, C. Uzoh and D.J. Pearson, "Copper Interconnection Integration and Reliability", *Thin Solid Films*, Vol. 262, pp. 84-92, 1995.
- [6] K.-W. Kwon, C. Ryu, S.S. Wong and R. Sinclair, "Evidence of heteroepitaxial growth of copper on beta-tantalum", *Applied Physics Letters*, Vol. 71, No. 21, pp. 3069-3071, 24 November 1997.

- [7] C. Ryu, H. Lee, K.-W. Kwon, A.L.S. Loke, and S.S. Wong, "Barriers for copper interconnections", *Solid State Technology*, Vol. 42, No. 4, pp. 53-56, April 1999.
- [8] T. Nitta, T. Ohmi, T. Hsohi, S.Saki, K. Sakaibara, S. Imai, and T. Shibata, "Evaluating the large electromigration resistance of copper interconnects employing a newly developed accelerated life-test method", *Journal of the Electrochemical Society*, Vol. 140, pp. 1131-1137, 1993.
- [9] C.K. Hu, B. Luther, F.B. Kaufman, J. Hummel, C. Uzoh, and D.J. Rerson, "Copper interconnection integration and reliability", *Thin Solid Films*, Vol. 262, Issue. 1/2, pp. 84-92, 15 June 1995.
- [10] M. Shatzkes and J.R.Lloyd, "A model for conductor failure considering diffusion concurrently with electromigration resulting in a current exponent of 2", *Journal of Applied Physics*, Vol. 59, No. 11, pp.3890-3893, 1 June 1986.
- [11] A.K. Kulkarni, L.C. Chang, "Electrical and structural characteristics of chromium thin films deposited on glass and alumina substrates", *Thin Solid Films*, Vol. 301, pp. 17-22, 1997.
- [12] G. Palasantzas, Y.P. Zhao, G.C. Wang, T.M. Lu, J. Barnas, J.Th.M. De Hosson, "Electrical conductivity and thin-film growth dynamics", *Physical Review B-Condensed Matter*, Vol. 61, No. 16, pp.11109-11117, April 2000.
- [13] T. Oku, E. Kawakami, M. Uekubo, K. Takahiro, S. Yamaguchi, and M. Murakami, "Diffusion barrier property of TaN between Si and Cu", *Applied Surface Science*, Vol. 99, pp. 265-272, 1996.
- [14] K. Holloway, P.M. Fryer, C. Cabral, J.M.E. Harper, P.J. Bailey, and K.H. Kelleher, "Tantalum as a diffusion barrier between copper and silicon: Failure mechanism and effect of nitrogen additions", *Journal of Applied Physics*, Vol. 71, No. 11, pp. 5433-5444, June 1992.
- [15] H.J. Lee, K.W. Kwon, C.Ryu, and R. Sinclair, "Thermal stability of a Cu/Ta multilayer: An intriguing interfacial reaction", *Acta mater*, Vol. 47, No. 15, pp. 3965-3975, 1999.
- [16] C. Apblett, D. Muira, M. Sullivan, and P.J. Ficalora, "Reaction of Cu-Ti bilayer films in vacuum and hydrogen", *Journal of Applied Physics*, Vol. 71, No. 10, pp. 4925-4932, 15 May 1992.
- [17] K.P. Rodbell, P.J. Ficalora, "The role of hydrogen in altering the electrical properties of gold, titanium, and tungsten films", *Journal of Applied Physics*, Vol. 65, No. 8, pp. 3107-3117, 15 April 1989.
- 圖 6 Cu/Ta/SiO<sub>2</sub> 結構之相對電阻對電流密度之函數。
- 圖 7 Cu/Ta/SiO<sub>2</sub> 結構之溫度上升對電流密度之函數。
- 圖 8 Cu/Ta/SiO<sub>2</sub> 結構之相對電阻對時間之變化, 測試電流密度為 5 MA/cm<sup>2</sup>。
- 圖 9 Cu/Ta/SiO<sub>2</sub> 結構之活化能。
- 圖 10 AFM 表面之形態(a)SiO<sub>2</sub>(b)HSQ。
- 圖 11 銅(111)在剛沈積之 XRD(a)Cu/Ta/SiO<sub>2</sub>/Si (b) Cu/Ta/HSQ/Si (c)Cu/SiO<sub>2</sub>/Si。
- 圖 12 Cu/Ta/HSQ 結構在退火後, 可能產生的化學反應, 相轉換及其所在位置。
- 圖 13 Cu/Ta/HSQ 結構之 XRD。
- 圖 14 HSQ/Cu/Ta/HSQ 結構之二次離子質譜儀縱深元素分佈圖。
- 圖 15 Cu/Ta/HSQ 結構之活化能。

#### 圖目錄

- 圖 1 HSQ 在氮氣中的熱重/熱差分析, 加熱速率為 10 °C/分鐘。
- 圖 2 HSQ 在不同溫度的傅立葉轉換紅外光譜。
- 圖 3 HSQ 在不同溫度的折射率。
- 圖 4 二次離子質譜儀縱深元素分佈圖在 400°C, 1 小時退火處理(a)HSQ/Cu/HSQ (b)HSQ/Cu/Ta/HSQ。
- 圖 5 Cu/Ta/SiO<sub>2</sub> 結構之電阻對溫度之函數。

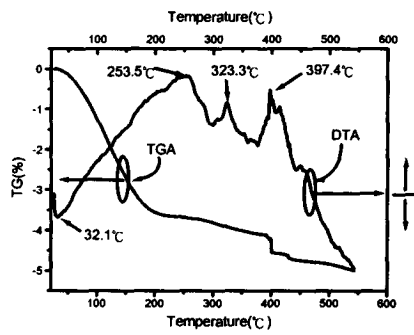


圖1 HSQ在氮氣中的熱重/熱差分析，加熱速率為10°C/分鐘。

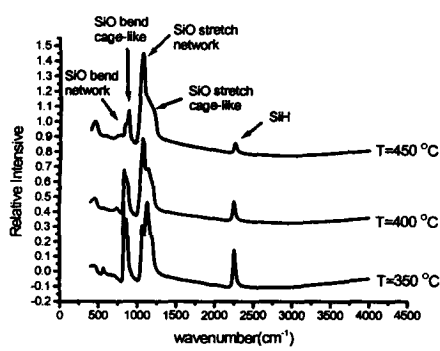


圖2 HSQ在不同溫度的傅立葉轉換紅外光譜。

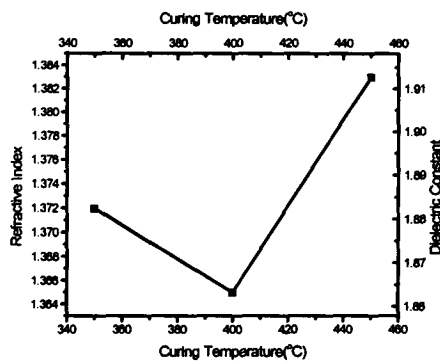
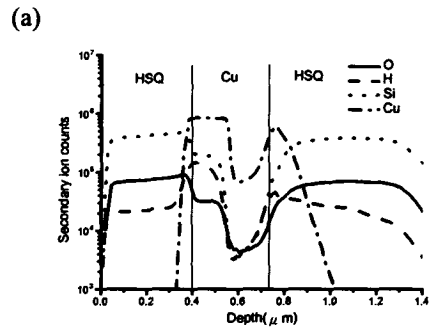
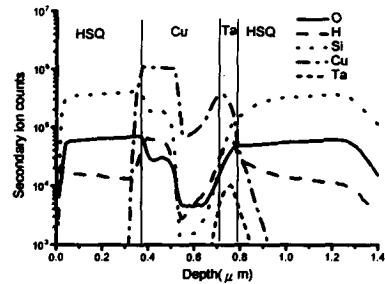


圖3 HSQ在不同溫度的折射率。



(a)



(b)

圖4 二次離子質譜儀縱深元素分佈圖在400°C, 1小時退火處理(a)HSQ/Cu/HSQ (b)HSQ/Cu/Ta/HSQ。

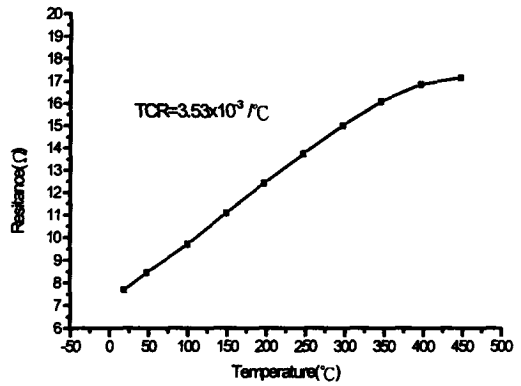


圖5 Cu/Ta/SiO<sub>2</sub>結構之電阻對溫度之函數。

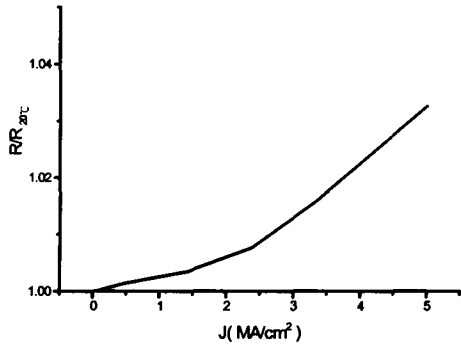


圖6 Cu/Ta/SiO<sub>2</sub>結構之相對電阻對電流密度之函數。

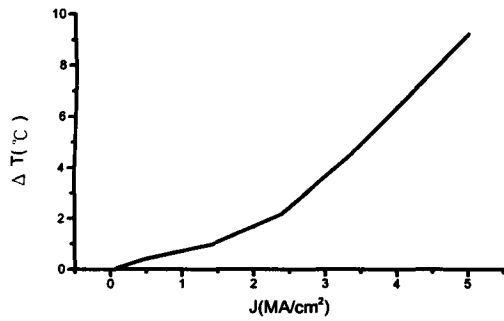


圖7 Cu/Ta/SiO<sub>2</sub>結構之溫度上升對電流密度之函數。

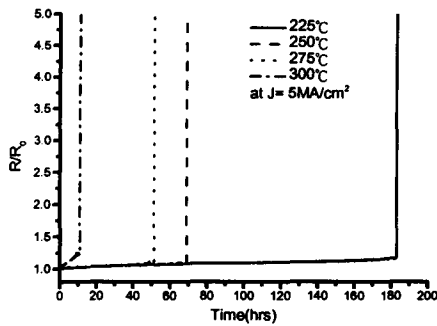


圖8 Cu/Ta/SiO<sub>2</sub>結構之相對電阻對時間之變化，測試電流密度為5 MA/cm<sup>2</sup>。

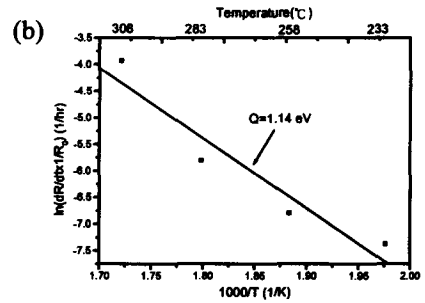
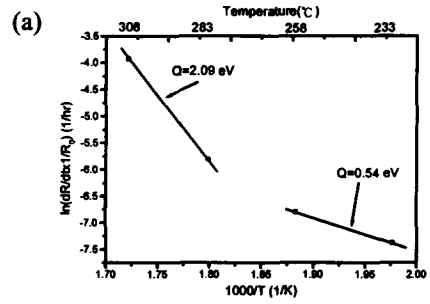
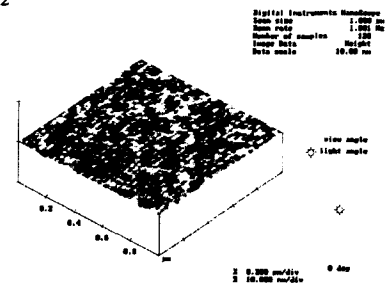


圖9 Cu/Ta/SiO<sub>2</sub>結構之活化能。

(a) SiO<sub>2</sub>



(b) HSQ

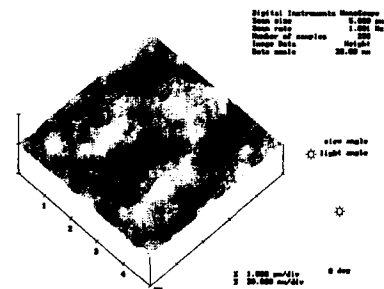


圖10 AFM表面之形態(a)SiO<sub>2</sub>(b)HSQ。

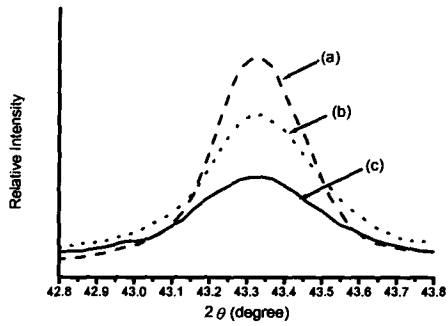


圖11 銅(111)在剛沈積之XRD(a)Cu-Ta/SiO<sub>2</sub>/Si (b) Cu-Ta/HSQ/Si (c)Cu/SiO<sub>2</sub>/Si。

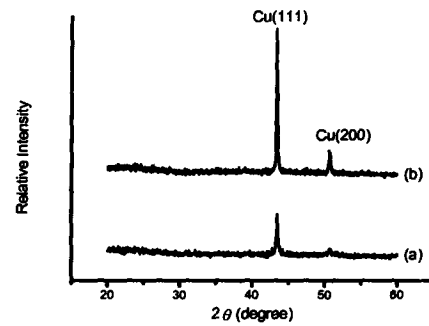


圖13 Cu-Ta/HSQ結構之XRD。

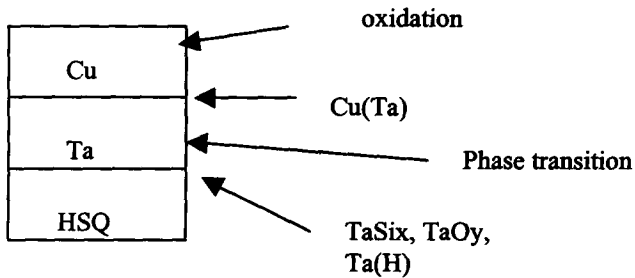
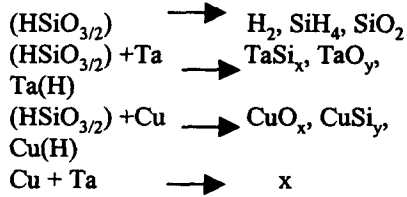


圖12 Cu-Ta/HSQ結構在退火後，可能產生的化學反應，相轉換及其所在位置。

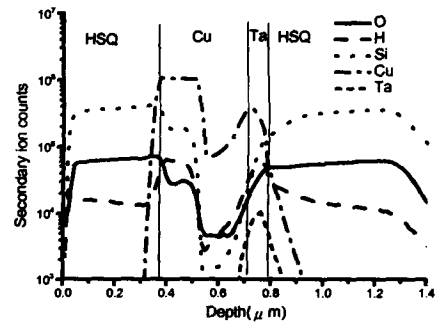


圖14 HSQ/Cu-Ta/HSQ結構之二次離子質譜儀縱深元素分佈圖。

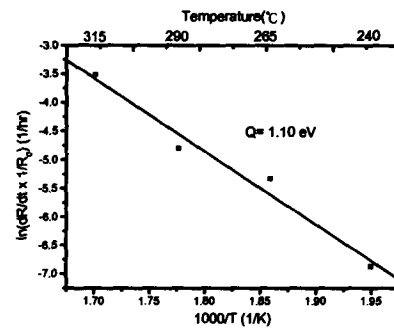


圖15 Cu-Ta/HSQ結構之活化能。